JPEDAV (2004) 25:520-527
DOI: 10.1361/15477020421043
1547-7037/$19.00 ©ASM International

Thermodynamic Evaluation of the Al-H System

Caian Qiu, Gregory B. Olson, Susanne M. Opalka, and Donald L. Anton

(Submitted February 2, 2004; in revised form August 31, 2004)

The thermodynamic properties of the Al-H system were assessed using models for the Gibbs energy of the individual phases, including the metastable hydride AlH_3 phase. The model parameters were obtained through optimization by best fitting to selected experimental data. Particular attention was paid to hydrogen solubility in liquid and face-centered-cubic (fcc) Al. It was shown that the hydrogen can be treated as an ideal gas under normal conditions. The hydrogen solubility in liquid and fcc Al can be described very well with a regular solution model for liquid and fcc. The present calculations show satisfactory agreement with most experimental data for hydrogen solubility in fcc Al and selected data for hydrogen solubility in liquid Al, qualifying the extension of this binary model to higher-order Al-H-bearing systems.

1. Introduction

The binary Al-H diagram is simple with a eutectic reaction liquid(Al) → face-centered-cubic (fcc)(Al) + H_2(gas) near the melting temperature of Al, as proposed by San-Martin and Manchester (Ref 1). The hydrogen solubility in both liquid and fcc Al is very small, approximately 0.001 and 0.0001 at.% at the melting temperature at 1 atm. No stable hydride has been observed in the Al-H system, but a metastable AlH_3 prepared under high pressures (10^9 Pa) was reported. When modeling sodium alanates ($NaAlH_4$ and Na_3AlH_6) in the Al-Na-H system, it was found by the present authors that thermodynamic modeling is not available for the Al-H system. Consequently, this was pursued in the present work.

Dissolution of hydrogen in Al and Al-based alloys, even if in a very small amount, can exert strong effects on their mechanical properties. Numerous experiments have been carried out to examine the hydrogen solubility in liquid Al, solid Al, and its alloys, under different conditions, as reviewed in Ref 1 and 2. The measurements from different investigators do not agree well with one another. The purpose of the present work is to assess the thermodynamic properties of the Al-H system by taking all experimental information into account and then to obtain a consistent thermodynamic description to support the modeling of the ternary Al-Na-H system (Ref 3).

2. Thermodynamic Modeling

The four phases in the Al-H system: gas, liquid, fcc solid solution, and metastable hydride AlH_3 with hexagonal structure (Ref 1) were treated with different thermodynamic models in the present work. The models describe the Gibbs energy for each phase as a function of temperature, composition, and pressure (only for the gaseous phase).

The liquid phase is modeled as a substitutional solution between Al and H, and its molar Gibbs energy is given by

$$G_m^{liq} = x_{Al}\,{}^{o}G_{Al}^{liq} + x_H\,{}^{o}G_H^{liq} + RT(x_{Al}\ln x_{Al} + x_H \ln x_H) + x_{Al}x_H L \quad \text{(Eq 1)}$$

where x_i is the mole fraction of Al or H, and ${}^{o}G_i^{liq}$ is the Gibbs energy of Al or H in liquid state, referred to the enthalpy of the so-called stable element reference (SER) at 298.15 K and 1 bar (same thereafter). The quantity of ${}^{o}G_{Al}^{liq}$ has been evaluated (Ref 4) based on experimental information, but ${}^{o}G_H^{liq}$ is not well known because liquid hydrogen exists only at extremely low temperatures (from 14 to 21 K) (Ref 5). Consequently, ${}^{o}G_H^{liq}$ was estimated from the experimental solubility of hydrogen in liquid Al and liquid Na in conjunction with the binary Na-H system (Ref 6).

The first two terms in Eq 1 represent a mechanical mixture of the pure elements, the third is the contribution from mixing entropy, and the last is excess energy due to the interaction between Al and H in the liquid describing its nonideal behavior. The interaction parameter L is expressed as a linear function of temperature, $L = A + BT$ and is to be evaluated from relevant experimental data.

Hydrogen atoms are much smaller than those of aluminum and can occupy the interstitial sites of fcc Al. Due to the lack of direct experimental measurement, it was assumed that hydrogen atoms occupy the octahedral interstitial sites in fcc Al, in which the number of the interstitial sites is the same as that of lattice sites of Al atoms. As a consequence, the solid-solution fcc is described as an interstitial solution with the formula $(Al)_1(H,Va)_1$, where Al atoms occupy the first sublattice, while hydrogen atoms and vacancies (Va) enter into the second one. According to this model, the Gibbs energy for one molar formula unit of $(Al)_1(H,Va)_1$ is expressed as

$$G_m^{fcc} = y_H\,{}^{o}G_{Al:H}^{fcc} + y_{Va}\,{}^{o}G_{Al:Va}^{fcc} + RT(y_H \ln y_H + y_{Va}\ln y_{Va}) + G_m^{ex} \quad \text{(Eq 2)}$$

with

$$G_m^{ex} = y_H y_{Va}[L_0 + (y_H - y_{Va})L_1 + (y_H - y_{Va})^2 L_2 + \ldots] \quad \text{(Eq 3)}$$

Caian Qiu, QuesTek Innovations LLC, 1820 Ridge Ave., Evanston, Illinois 60201; **Gregory B. Olson,** Department of Materials Science and Engineering, Northwestern University, Evanston, Illinois 60201, also with QuesTek Innovations; and **Susanne M. Opalka** and **Donald L. Anton,** United Technology Research Center, 411 Silver Lane, East Hartford, Connecticut 06084. Contact e-mail: cqui@questek.com.

Here y_H and y_{Va} are site-fractions of hydrogen atoms and vacancies, respectively, and they follow the relation $y_H + y_{Va} = 1$. The quantity $^{\circ}G^{fcc}_{Al:Va}$ is the Gibbs energy of pure Al in fcc structure, and $^{\circ}G^{fcc}_{Al:H}$ is the Gibbs energy of a hypothetical state where all the interstitial sites in fcc Al are filled with hydrogen. Without relevant experimental information, the Gibbs energy of AlH in the fcc structure was set as follows in order for AlH to maintain the metastability relative to fcc Al and hydrogen gas:

$$^{\circ}G^{fcc}_{Al:H} = 10{,}000 + {^{\circ}G^{fcc}_{Al}} + 0.5\ {^{\circ}G^{gas}_{H2}} \qquad \text{(Eq 4)}$$

The interaction parameters L_0, L_1, and L_2 in Eq 3 are to be evaluated from the experimental data of hydrogen solubility in fcc Al.

The metastable hydride AlH_3 is treated with the two-sublattice model, $(Al)_1(H)_3$, and the Gibbs energy for one mole of formula unit is given by

$$^{\circ}G^{Al3H}_{m} = a + bT + cT \ln T + dT^2 + \ldots + e/T \qquad \text{(Eq 5)}$$

Its enthalpy H_m, entropy S_m, and heat capacity C_p can be derived from Eq 5 as

$$H_m = \partial(G_m/T)/\partial(1/T) = a - cT - dT^2 - 2eT^3 + \ldots + 2f/T \qquad \text{(Eq 6a)}$$

$$S_m = -\partial G_m/\partial T = -b - c(1 + \ln T) - 2dT^2 - 3eT^3 + \ldots + f/T^2 \qquad \text{(Eq 6b)}$$

$$C_p = \partial H_m/\partial T = -c - 2dT - 6eT^3 + \ldots -2f/T^2 \qquad \text{(Eq 6c)}$$

It has been shown that hydrogen gas deviates from the ideal gas behavior at very high pressures, but it can be approximated as an ideal gas under normal conditions (Ref 7). The ideal gas model was applied to the gaseous phase composed of Al, AlH, AlH_2, AlH_3, Al_2, H, and H_2, with H_2 as the dominant species in most cases. The interaction among various species was neglected in the present model. Its molar Gibbs energy is expressed as a function of temperature:

$$G^{gas}_{m} = \sum_i [x_i\ {^{\circ}G^{gas}_{i}} + RTx_i \ln x_i]$$
$$i = \text{Al, AlH, AlH}_2\text{, AlH}_3\text{, Al}_2\text{, H, and H}_2 \qquad \text{(Eq 7)}$$

where x_i is the mole fraction of each species in the gaseous phase, and $^{\circ}G^{gas}_{i}$ is the molar Gibbs energy of each species expressed by Eq 5 with an additional term $RT \ln P$ [P is pressure in bar (10^5 Pa)]. Their descriptions were taken from the Scientific Group Thermodata Europe (SGTE) database (Ref 8), which is based on the JANAF Tables (Ref 9).

3. Experimental Information and Model Evaluation

There are numerous experimental measurements of the hydrogen solubility in liquid and solid Al (Ref 10-20), and results clearly show that the solubility C_H in liquid or fcc Al obeys Sieverts' law:

$$C_H = C_o\sqrt{P}\exp\left[\frac{-\Delta H}{RT}\right] \qquad \text{(Eq 8)}$$

where C_o is a constant and P is pressure, T is temperature in Kelvin, and ΔH is the enthalpy of hydrogen solution in liquid or fcc Al. Most of the experimental data are presented as mL H_2 per 100 g Al, which can be converted to atomic percent through the standard state (1 mL volume hydrogen gas at 273 K and 1 atm) according to

$$H(\text{mL}/100\text{ g}) = \frac{273R \times H(\text{at.\%})}{2.01588 \times 10^{-6}\,P \times 26.9815} \qquad \text{(Eq 9)}$$

with

$P = 101{,}325$ Pa and $R = 8.31451$ J/K · mol

Table 1 Comparison of hydrogen solubility and enthalpy of solution ΔH in liquid and fcc Al from various studies

Authors	Year	Method	H in liquid, mL/100 g Al	ΔH, kJ/mol	H in fcc Al, mL/100 g Al	ΔH, kJ/mol
Ransley et al. (Ref 10)	1948	Sieverts	2.796-2760/T	52.84	0.788-2080/T	39.82
Opie et al. (Ref 11)	1950	Sieverts	2.62-2550/T	48.82	…	…
Eichenauer et al. (Ref 12)	1961	Saturation and extraction	2.969-3086/T	59.08	1.961-3042/T	58.24
Grigorenko et al. (Ref 13)	1967	Rapid quenching	2.528-2713/T	51.94	…	…
Eichenauer et al. (Ref 14)	1968	Saturation and extraction	…	…	2.105-3300/T	63.18
Ichimura et al. (Ref 15)	1979	Vacuum solid extraction	…	…	2.220-3340/T	63.94
Hashimoto et al. (Ref 16)	1983	Permeation and diffusion	…	…	4.976-5040/T	96.49
Feichtinger et al. (Ref 17)	1987	Rapid quenching	2.817-2970/T	56.86	…	…
Talbot et al. (Ref 18)	1988	Modified Sieverts	2.72-2700/T	51.69	…	…
Liu et al. (Ref 19)	1995	Sieverts	3.07-2980/T	57.05	…	…
Imabayashi et al. (Ref 20)	1995	Rapid quenching	2.256-2392/T	45.80	…	…

Note: The solubility is expressed with $\lg(C_H) = A + B/T$ in milliliters per 100 g Al at 1 atm, and ΔH is calculated according to$-8.3145B \times \ln 10$.

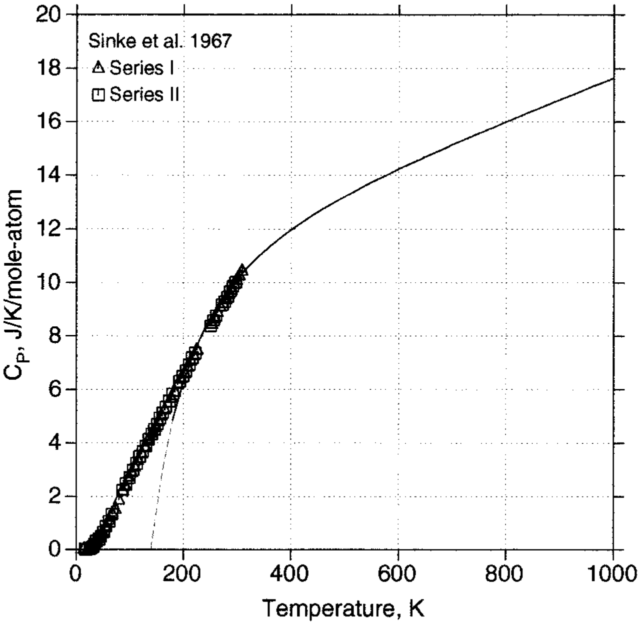

Fig. 1 Calculated heat capacity of AlH_3 in comparison with experimental data

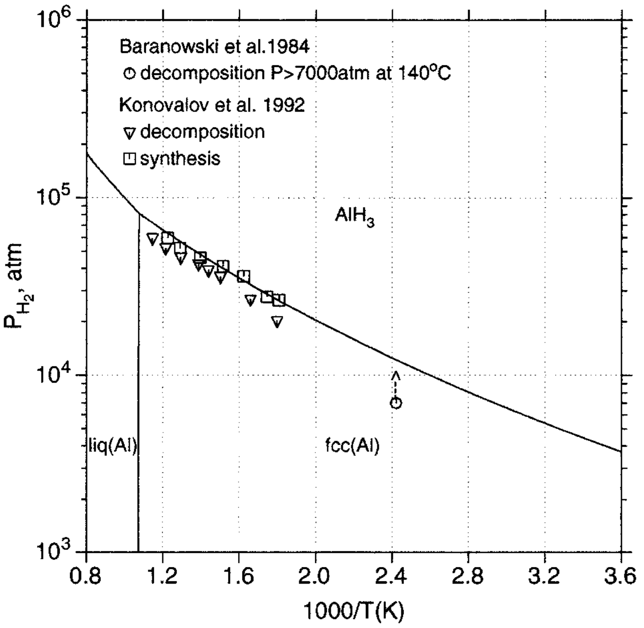

Fig. 3 Calculated phase stability diagram of the Al-H system, where the phase boundary between AlH_3 and fcc(Al) represents the dissociation pressure of AlH_3 in comparison with experimental data

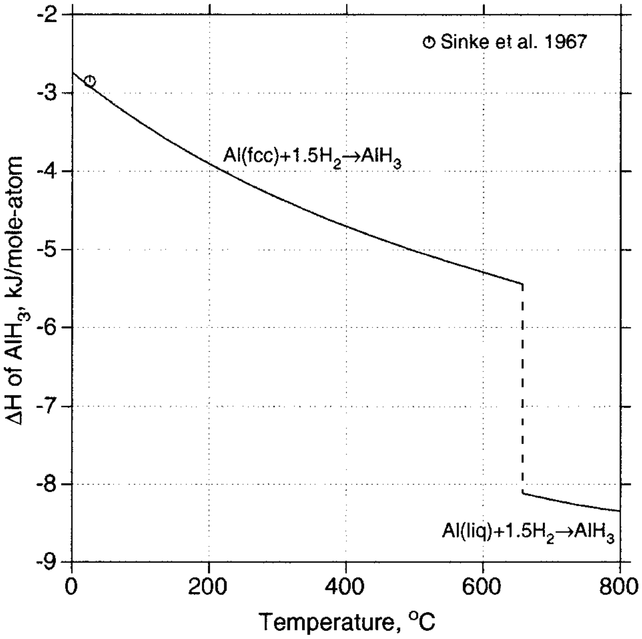

Fig. 2 Enthalpy of formation of AlH_3 calculated as a function of temperature in comparison with experimental data at 298.15 K

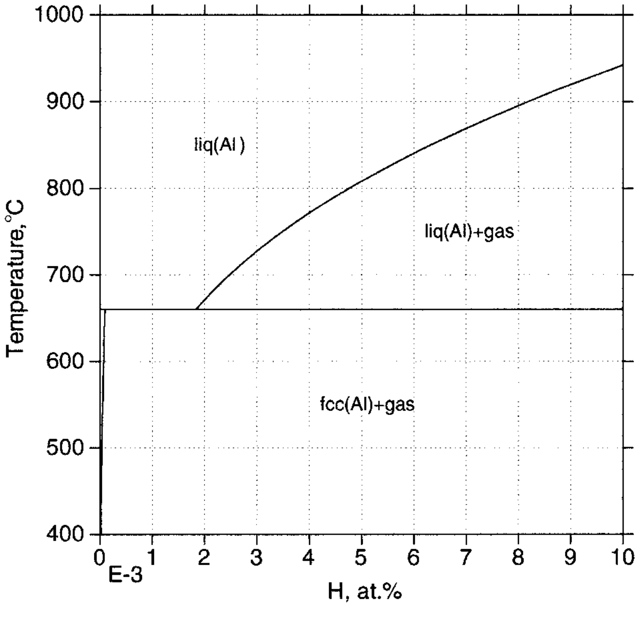

Fig. 4 Al-H phase diagram calculated at 1 atm

From Eq 8 it is seen that the hydrogen solubility will exhibit a linear relation with reciprocal temperature ($1/T$) in the Arrhenius plot:

$$\lg(C_H) = A + B/T + 0.5\lg(P) \qquad \text{(Eq 10)}$$

The solubility parameters derived from different experimental measurements are summarized in Table 1. By comparing Eq 10 and 8, it is found that the constant B is related to the enthalpy of solution of hydrogen in fcc or liquid Al, ΔH, as

$$\Delta H = -8.3145B \times \ln 10 \qquad \text{(Eq 11)}$$

Due to experimental difficulty and the possible complicating hydrogen absorption effects, the solubility measure-

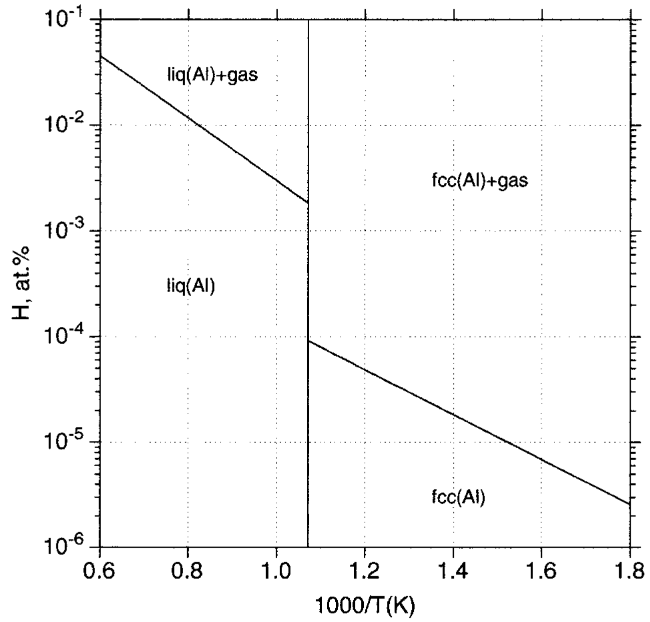

Fig. 5 Arrhenius plot of the Al-H diagram to show hydrogen solubility in liquid and fcc Al as a function of temperature at 1 atm

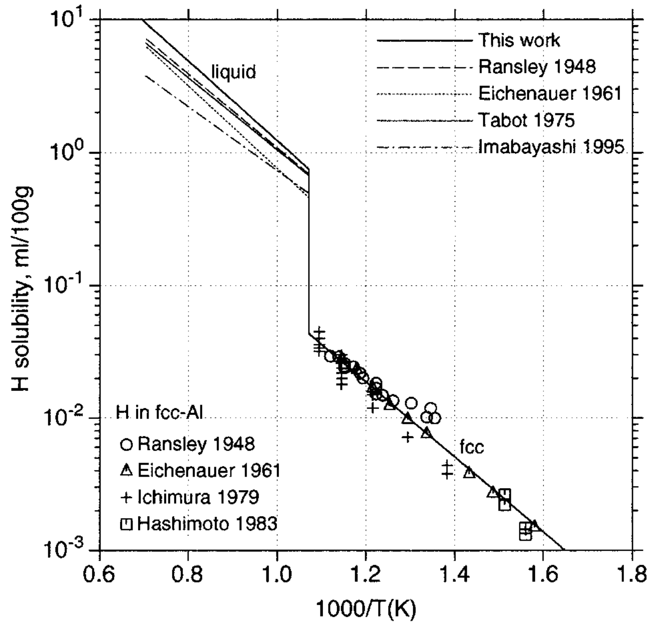

Fig. 6 Comparison between the present calculations and experimental information. The calculated solubility line in liquid coincides with the equation suggested by Liu et al. (Ref 19) based on their experimental measurements

ments from different investigators show certain discrepancies, as reviewed in Ref 1, 2, and 21.

With regard to the hydrogen solubility in liquid Al, the data from the literature (Ref 10, 11, 18) are very close to each other, and all others (Ref 12, 14, 17, 20) except Ref 19 show a lower solubility. In a recent work, Liu et al. found that inert gas (He or Ar) used in experiments contributed to the hydrogen solubility and was often ignored by other investigators (Ref 19). After taking such a contribution into account, their corrected data show the highest solubility. Their solubility data were selected in the current study to optimize the interaction parameter L in Eq 1 for liquid.

As for the hydrogen solubility in fcc Al, the results from Ref 10, 12, and 15 are consistent with each other over the temperature range from 500 to 600 °C, but the data from Eichenauer et al. (Ref 12) and Ichimura et al. (Ref 15) at temperatures below 500 °C fall below the extrapolation of the equation of Ransley et al. (Ref 10). The measurements by Eichenauer et al. (Ref 14) show a lower solubility compared with their previous data (Ref 12) and are probably caused by hydrogen trapping at defect sites in Al lattice, such as grain boundaries (Ref 21). From Table 1 it is noted that the solubility parameters proposed by Ichimura et al. (Ref 15) are very similar to those given by Eichenauer et al. (Ref 14). However, the data of Hashimoto et al. (Ref 16) differ significantly from others and appear to be unreliable because their measurements were made within a very narrow temperature range from 348 to 368 °C. Among these experimental data, Ref 10 and 12 are most frequently quoted in the literature and thus were selected for the present optimization to evaluate the excess Gibbs energy of the fcc solution in Eq 2.

In addition, a metastable hydride AlH_3 with a hexagonal structure has been reported. Its thermodynamic properties (enthalpy of formation and heat capacity) were studied by Sinke et al. (Ref 22), and its dissociation pressure was measured by Baranowski et al. (Ref 23, 24) and Konovalov et al. (Ref 25). There is a Gibbs energy description of AlH_3 in the substance database (SSUB) in Thermo-Calc (Ref 26) that does not reproduce the experimental data closely, especially the dissociation pressure. As a consequence, a new evaluation was made for AlH_3 according to Eq 5 based on these experimental data.

After selection of appropriate experimental data, the model parameters were optimized using the Thermo-Calc PARROT program. This can treat various types of input data simultaneously and optimize the parameters by searching for the best fit to selected experimental data. During the optimization, it was found that a regular solution model for liquid and fcc produced an excellent description of the hydrogen solubility in both liquid and fcc Al.

4. Results and Discussion

All the thermodynamic parameters describing the Al-H system are listed in the Appendix, which is used in the following to calculate the phase diagram and other thermodynamic properties.

The calculated molar heat capacity of AlH_3 is shown as a function of temperature in Fig. 1 and compared with the experimental measurements. It is seen that the calculations are in excellent agreement with the experimental data above 200 K, but cannot account for those data below 200 K due to the limitation of the present model. A different model (e.g., Debye model) would be necessary to model the heat capac-

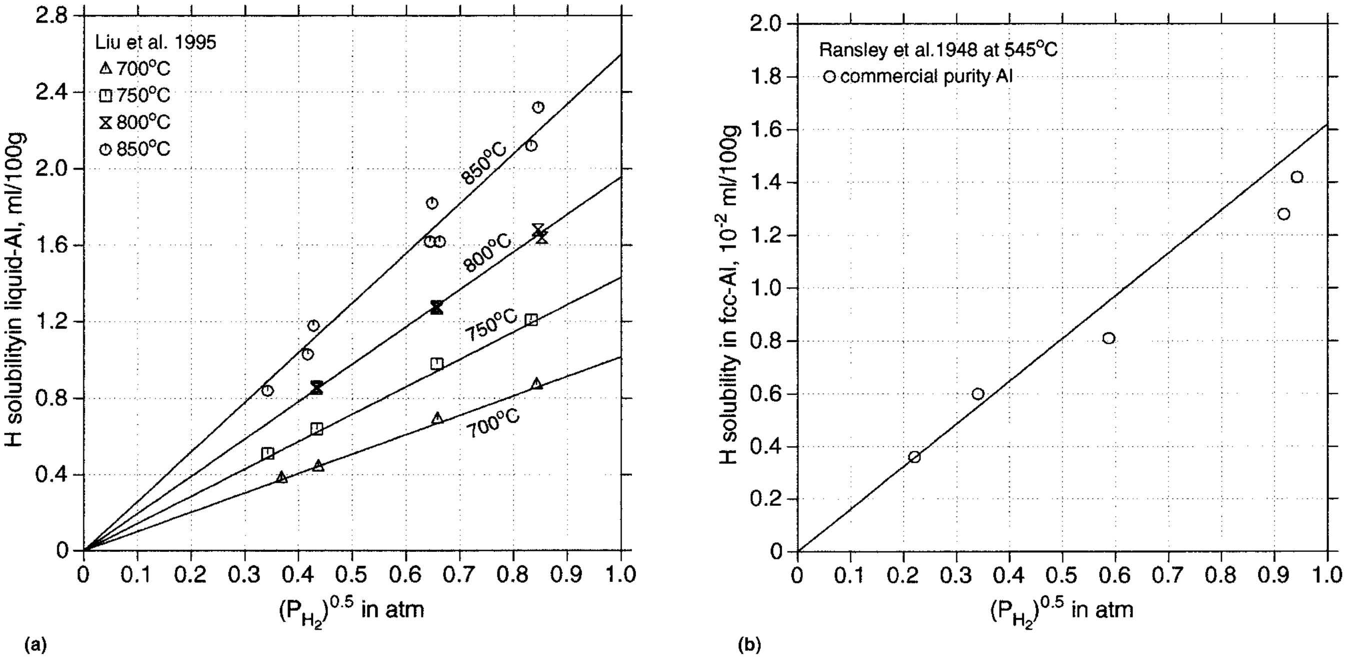

Fig. 7 Effect of pressure on the hydrogen solubility in **(a)** liquid Al and **(b)** fcc Al according to the present calculations and experimental data

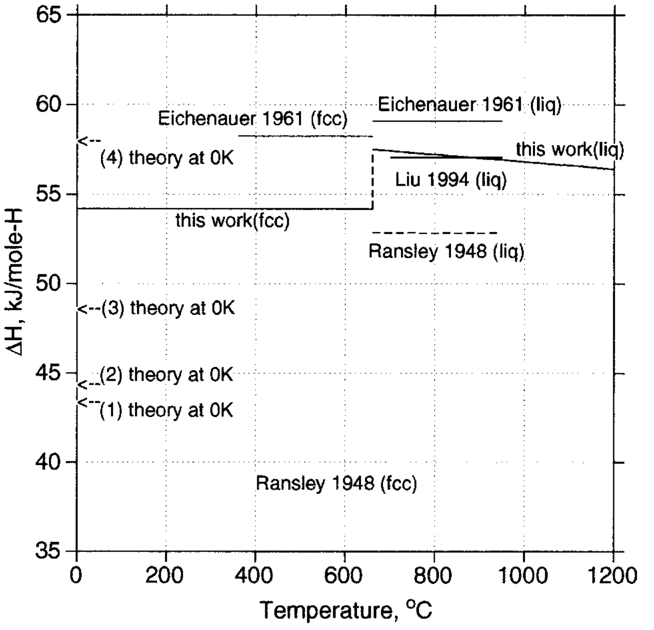

Fig. 8 Enthalpy of solution of hydrogen in fcc and liquid Al calculated at 1atm in comparison with some experimental data (Ref 10, 12, 19) and theoretical calculations at 0 K: (1) Popovic et al. (Ref 28), (2) Johnston et al. (Ref 29), (3) Mahajan et al. (Ref 30) for undilated lattice, (4) Mahajan et al. (Ref 30) for dilated lattice

ity at such low temperatures. This was not attempted in the present work.

According to the present modeling, the enthalpy of formation of AlH_3 changes with temperature, as illustrated in Fig. 2. The enthalpy of formation of AlH_3 calculated at 298.15 K and 1 bar is −2.92 kJ/mol atom, which agrees very well with experimental result −2.86 kJ/mol atom, obtained from measurements of the heat of decomposition and the heat capacity at low temperatures (Ref 22). A most recent theoretic prediction by Wolverton et al. (Ref 27) gives −3.76 kJ/mol atom based on first-principles calculations. They also predicted a strongly positive free energy of formation of the metastable AlH_3 at 300 K, 12.45 kJ/mol atom, which is consistent to the present calculation 7.92 kJ/mol atom.

A calculated phase stability diagram of the Al-H system is presented in Fig. 3. A single-phase area in Fig. 3 represents the temperature and hydrogen pressure ranges for the existence of stable phases. The phase boundary between fcc(Al) and AlH_3 represents the hydrogenation/dehydrogenation pressure and is compared with experimental data (Ref 23-25). From Fig. 3 it is seen that the present calculations are consistent with the experimental data, except a single data point at 140 °C from Ref 23. This data was obtained at an unknown pressure (higher than 7000 atm), and thus it is considered that the data are in line with the model prediction. From the comparison it is seen that the ideal-gas model is a good approximation in this case, although the dissociation pressure of AlH_3 is very high (GPa).

The calculated Al-H phase diagram at 1 atm is given in Fig. 4, showing a eutectic reaction liquid → fcc(Al) + gas(H_2) at 660 °C. An Arrhenius plot of the diagram is presented in Fig. 5 to show a linear relation between the hydrogen solubility in liquid or fcc Al and the reciprocal temperature (1/*T*).

As mentioned in Section 3, “Experimental Information and Model Evaluation,” there are numerous experimental data for the hydrogen solubility in liquid and solid Al. A comparison between the present modeling and experimental information is presented in Fig. 6. The solid line in Fig. 6 represents the present model prediction, and it coincides with the solubility equation suggested by Liu et al. based on their measurement of the hydrogen solubility in liquid Al (Ref 19). The calculated hydrogen solubility in fcc Al also shows satisfactory agreement with most of the experimental results from Ref 10, 12, 15, and 16. The data measured by Eichenauer et al., which are not shown in Fig. 6, fell slightly below the calculation because a certain portion of hydrogen was trapped at defect sites of Al lattice (Ref 14).

The pressure effect on the hydrogen solubility in liquid and fcc Al at different temperatures is illustrated in Fig. 7(a) and (b) according to the present calculations. These plots exhibit a linear relationship between the solubility and square root of pressure at a given temperature and are consistent with experimental data of Liu et al. (Ref 19) and Ransley et al. (Ref 10).

The enthalpy of solution of hydrogen in liquid and fcc Al, ΔH, was calculated at 1 atm in Fig. 8 compared with other experimental and theoretical data. It is seen that the calculated ΔH for liquid has a value of 57.505 kJ/mol atom at 660 °C and decreases slightly with increasing temperature. On the other hand, ΔH calculated for fcc remains almost constant, 54.195 kJ/mol atom. As discussed earlier, the calculated hydrogen solubility in liquid Al fit very well to the data from Liu et al. (Ref 19), while showing certain differences with others. As expected, the calculated enthalpy of solution of hydrogen shows the same trend when comparing with the corresponding experiments in Table 1. The enthalpy of solution of hydrogen in fcc Al varies significantly from different studies due to high uncertainty of experimental measurements at low temperatures. Theoretical predication at 0 K based on the assumption that hydrogen atoms occupy the octahedral interstitial sites in Al lattice with averaged interstitial charge density also varies from 44 to 58 kJ/mol atom (Ref 28-30). The present calculation is comparable with the experimental value obtained from the solubility equation of Eichenauer et al. (Ref 12). In addition, it is interesting to note that the authors' model calculation fell between the theoretical values calculated by Mahajan et al. (Ref 30) with and without Al lattice dilation.

5. Conclusions

The relevant experimental information of the binary Al-H system has been assessed with thermodynamic models. The models make use of the Gibbs energy of the individual phases, and the model parameters were obtained through optimization by best fit to selected experimental data. Thermodynamic properties of the metastable hydride AlH_3 were also modeled. Particular attention was paid to hydrogen solubility in liquid and fcc Al. It has been shown that the ideal-gas model is a good approximation to treat this solubility equilibria with liquid, fcc, or metastable AlH_3 under normal conditions. The hydrogen solubility in liquid and fcc Al can be described very well with a regular solution model for liquid and fcc. Calculations from the present modeling account very well for most experimental data (Ref 10, 12, 15, 16) for hydrogen solubility in fcc Al and also show satisfactory agreement with the data by Liu et al. (Ref 19) for hydrogen solubility in liquid Al.

Acknowledgment

This work was financially supported by the United States Department of Energy under Contract No. DE-FC04-02AL67610, managed by United Technology Research Center, East Hartford, CT. The authors would like to thank Prof. M. Asta at Northwestern University in Evanston, IL, for providing Ref 27.

Appendix

Summary of Thermodynamic Parameters Describing the Al-H System

Values are given in SI units (Joule, mole, Kelvin, and Pa) and correspond to one mole of formula units of the phases. The parameters marked with an asterisk (*) were evaluated in the present work.

Liquid formula (Al,H)

$$^{\circ}G_{\mathrm{Al}}^{\mathrm{liq}} = 11{,}005.553 - 11.840873T + 7.9401 \times 10^{-20}\, T^{7} + \mathrm{GHSERAL} \qquad 298.15 < T < 933.60$$

$$= 10{,}481.974 - 11.252014T + 1.234264 \times 10^{28}\, T^{-9} + \mathrm{GHSERAL} \qquad 933.60 < T < 2900.00$$

$$^{\circ}G_{\mathrm{H}}^{\mathrm{liq}} = 8035 + 25T + 2T \ln(T) + 0.5 \times \mathrm{F10{,}784}T \qquad (*)$$

$$L_{\mathrm{Al,H}}^{\mathrm{liq}} = 51{,}338 - 11.4758T \qquad (*)$$

fcc_Al with formula $(Al)_1(H,Va)_1$

$$^{\circ}G_{\mathrm{Al:H}}^{\mathrm{fcc}} = 100{,}000 + \mathrm{GHSERAL} + 0.5 \times \mathrm{F10{,}784}T \qquad (*)$$

$$^{\circ}G_{\mathrm{Al:Va}}^{\mathrm{fcc}} = \mathrm{GHSERAL}$$

$$L_{\mathrm{Al,H}}^{\mathrm{fcc}} = -45{,}805 + 56.4302T \qquad (*)$$

AlH_3 with formula $(Al)_1(H)_3$

$$^{\circ}G_{\mathrm{Al:H}}^{\mathrm{AlH3}} = -28{,}415 + 213.712933T - 41.75632T \ln(T) - 0.0145484697T^{2} + 446{,}400/T \qquad (*)$$

Gas with formula (Al, Al1H1, Al1H2, Al1H3, Al2, H, H2)

$$^{\circ}G_{\mathrm{Al}}^{\mathrm{gas}} = \mathrm{F154}T + RT \ln(10^{-5} P)$$

$$^{\circ}G_{\mathrm{Al1H1}}^{\mathrm{gas}} = \mathrm{F448}T + RT \ln(10^{-5} P)$$

$$^{\circ}G_{\mathrm{Al1H2}}^{\mathrm{gas}} = \mathrm{F484}T + RT \ln(10^{-5} P)$$

$$^{\circ}G_{\mathrm{Al1H3}}^{\mathrm{gas}} = \mathrm{F498}T + RT \ln(10^{-5} P)$$

$$^{\circ}G^{\mathrm{gas}}_{\mathrm{Al2}} = \mathrm{F625}T + RT\ln(10^{-5}\,P)$$

$$^{\circ}G^{\mathrm{gas}}_{\mathrm{H}} = \mathrm{F10383}T + RT\ln(10^{-5}\,P)$$

$$^{\circ}G^{\mathrm{gas}}_{\mathrm{H2}} = \mathrm{F10784}T + RT\ln(10^{-5}\,P)$$

Symbols:

GHSERAL

$−7976.15 + 137.071542T − 24.3671976T\ln(T)$
$− 0.001884662T^2 − 8.77664 \times 10^{-7}\,T^3$
$+ 74{,}092/T \qquad 298.15 < T < 700.00$

$−11{,}276.24 + 223.02695T − 38.5844296T\ln(T)$
$+ 0.018531982T^2 − 5.764227 \times 10^{-6}\,T^3$
$+ 74{,}092/T \qquad 700.00 < T < 933.60$

$−11{,}277.683 + 188.661987T − 31.748192T\ln(T)$
$− 1.234264 \times 10^{28}\,T^{-9} \qquad 933.60 < T < 2900.00$

F154*T*

$+323{,}947.58 − 25.1480943T − 20.859T\ln(T)$
$+ 4.5665 \times 10^{-5}\,T^2 − 3.942 \times 10^{-9}\,T^3$
$− 24{,}275.5/T \qquad 298.15 < T < 4300.00$

$+342{,}017.233 − 54.0526109T − 17.7891T\ln(T)$
$+ 6.822 \times 10^{-5}\,T^2 − 1.91111667 \times 10^{-8}\,T^3$
$− 14{,}782{,}200/T \qquad 4300.00 < T < 8200.00$

$+542{,}396.07 − 411.214335T + 22.2419T\ln(T)$
$− 0.00349619$

$T^2 + 4.0491 \times 10^{-8}\,T^3 − 2.0366965 \times 10^{8}/T$
$8200.00 < T < 10{,}000.00$

F448*T*

$+242{,}339.885 − 33.8756936T − 22.30163T\ln(T)$
$− 0.009810825\,T^2 + 1.170884 \times 10^{-6}\,T^3$
$− 81867.35/T \qquad 298.15 < T < 1000.00$
$+229{,}237.958 + 91.6810894T − 40.27554T\ln(T)$
$+ 0.0014274115T^2 − 1.87539833 \times 10^{-7}\,T^3$
$+ 1{,}742{,}835.5/T \qquad 1000.00 < T < 2900.00$
$+362{,}863.848 − 449.840707T + 27.45815T\ln(T)$
$− 0.01376392T^2 + 4.48236333 \times 10^{-7}\,T^3$
$− 47{,}477{,}990/T \qquad 2900.00 < T < 5400.00$
$−239{,}497.096 + 1079.59411T − 151.9828T\ln(T)$
$+ 0.0100311T^2 − 1.43955783 \times 10^{-7}\,T^3$
$+ 3.3253275\mathrm{E} + 08/T \qquad 5400.00 < T < 6000.00$

F484*T*

$+268{,}822.747 − 48.4999117T − 23.05794T\ln(T)$
$− 0.02008776T^2 + 2.30495167 \times 10^{-6}\,T^3$
$− 87{,}501.45/T \qquad 298.15 < T < 1000.00$
$+249{,}509.094 + 146.734812T − 51.21688T\ln(T)$
$− 0.0017335735T^2 + 4.76313167 \times 10^{-8}\,T^3$
$+ 2{,}409{,}628/T \qquad 1000.00 < T < 4900.00$
$+209{,}682.685 + 249.162251T − 63.23662T\ln(T)$
$− 1.554914 \times 10^{-4}\,T^2 + 9.71094833 \times 10^{-9}\,T^3$
$+ 26{,}656{,}905/T \qquad 4900.00 < T < 6000.00$

F498*T*

$+121{,}005.101 − 73.481737T − 16.47986T\ln(T)$
$− 0.041763035T^2 + 5.34620833 \times 10^{-6}\,T^3$
$− 67{,}626.8/T \qquad 298.15 < T < 800.00$
$+95{,}829.9422 + 215.650994T − 59.0983T\ln(T)$
$− 0.009502295T^2 + 7.25739 \times 10^{-7}\,T^3$
$+ 2{,}730{,}741/T \qquad 800.00 < T < 1800.0$
$+70{,}435.6419 + 385.238284T − 81.99149T\ln(T)$
$− 1.761597 \times 10^{-4}\,T^2 + 4.99483 \times 10^{-9}\,T^3$
$+ 8{,}127{,}570/T \qquad 1800.00 < T < 6000.00$

F625*T*

$+496{,}408.232 + 35.479739T − 41.6397T\ln(T)$
$+ 0.00249636T^2 − 4.90507333 \times 10^{-7}\,T^3$
$+ 85{,}390.3/T \qquad 298.15 < T < 900.00$
$+497{,}613.221 + 17.368131T − 38.85476T\ln(T)$
$− 2.249805 \times 10^{-4}\,T^2 − 9.49003167 \times 10^{-9}\,T^3$
$− 5287.23/T \qquad 900.00 < T < 2800.00$

F10383*T*

$+211{,}801.621 + 24.4989821T − 20.78611T\ln(T)$

F10784*T*

$−9522.9741 + 78.5273879T − 31.35707T\ln(T)$
$+ 0.0027589925T^2 − 7.46390667 \times 10^{-7}\,T^3$
$+ 56{,}582.3/T \qquad 298.15 < T < 1000.00$
$+180.108664 − 15.6128256T − 17.84857T\ln(T)$
$− 0.00584168T^2 + 3.14618667 \times 10^{-7}\,T^3$
$− 1{,}280{,}036/T \qquad 1000.00 < T < 2100.00$
$−18{,}840.1663 + 92.3120255T − 32.05082T\ln(T)$
$− 0.0010728235T^2 + 1.14281783 \times 10^{-8}\,T^3$
$+ 3{,}561{,}002.5/T \qquad 2100.00 < T < 6000.00$

References

1. A. San-Martin and F.D. Manchester, The Al-H System, *J. Phase Equilibria,* Vol 13, 1992, p 17-21
2. D.E.J. Talbot, Effects of Hydrogen in Aluminum, Magnesium, Copper, and Their Alloys, *Int. Metall. Rev.,* Vol 20, 1975, p 166-184
3. C. Qiu, G.B. Olson, S. Opalka, and D.L. Anton, Thermodynamic Modeling of Sodium Alanates, to be published
4. A. Dinsdale, SGTE Data for Pure Elements, *CALPHAD,* Vol 15, 1991, p 317-425

5. H.M. Roder, The H_2 System, *Bull. Alloy Phase Diagrams,* Vol 2, 1981, p 362-366
6. C. Qiu, G.B. Olson, S. Opalka, and D.L. Anton, A Thermodynamic Assessment of the Na-H System, to be published
7. H. Sugimoto and Y. Fukai, Solubility of Hydrogen in Metals Under High Hydrogen Pressures: Thermodynamical Calculations, *Acta Metall. Mater.,* Vol 40, 1992, p 2327-2336
8. I. Ansara and B. Sundman, *Computer Handling and Dissemination of Data,* P.S. Glaeser, Ed., North-Holland, 1987, p 154-158
9. M.W. Chase, Jr., C.A. Davies, J.R. Downey, Jr., D.J. Furip, R.A. McDonald, and A.N. Syverud, JANAF Thermochemical Tables, 3rd ed., J. Phys. Chem. Ref. Data, 1985, Vol 14, Suppl. 1
10. C.E. Ransley and D.E. Neufeld, The Solubility of Hydrogen in Liquid and Solid Aluminum, *J. Inst. Met.,* Vol 74, 1948, p 599-604
11. W.R. Opie and N.J. Grant, Hydrogen Solubility in Aluminum and Some Aluminum Alloys, *Trans. AIME,* Vol 188, 1950, p 1237-1247
12. V.W. Eichenauer, K. Hattenbach, and A. Pebler, The Solubility of Hydrogen in Solid and Liquid Aluminum, *Z. Metallkde.,* Vol 52, 1961, p 682-684 (in German)
13. G.M. Grigorenko and V.I. Lakomsky, Solubility of Hydrogen in Aluminum at Temperatures Characteristic of Arc Melting, *Auto. Weld.,* Vol 20, 1967, p 27-29
14. V.W. Eichenauer, The Solubility of Hydrogen and Deuterium in Extremely Pure Aluminum at Temperature Ranging from 400 to 600°C, *Z. Metallkde.,* Vol 59, 1968, p 613-616 (in German)
15. M. Ichimura, M. Imabayashi, and M. Hayakawa: Measurement of the Diffusion Coefficient and Solubility of Hydrogen in Solid Aluminum, *J. Jpn. Inst. Met.,* Vol 43, 1979, p 876-883 (in Japanese)
16. E. Hashimoto and T. Kino, Hydrogen Diffusion in Aluminum at High Temperatures, *J. Phys. F: Met. Phys.,* Vol 13, 1983, p 1157-1165
17. H. Feichtinger and R.A. Morach, Solubility of Hydrogen in Molten Aluminum at High Pressures, *Aluminium,* Vol 63, 1987, p 181-187 (in German)
18. D.E.J. Talbot and P.N. Anyalebechi, Solubility of Hydrogen in Liquid Aluminum, *Mater. Sci. Technol.,* Vol 4, 1988, p 1-4
19. H. Liu, M. Bouchard, and L. Zhang, An Experimental Study of Hydrogen Solubility in Liquid Aluminum, *J. Mater. Sci.,* Vol 30, 1995, p 4309-4315
20. M. Imabayashi, M. Ichimura, and Y. Sasajima, Solubility of Hydrogen in Molten Aluminum, *Keikinzoku (Light Metals),* Vol 45, 1995, p 278-283 (in Japanese)
21. J.R. Scully, G.A. Young, Jr., and S.W. Smith, Hydrogen Solubility, Diffusion and Trapping in High Purity Aluminum and Selected Al-based Alloys, *Mater. Sci. Forum,* Vol 331-337, 2000, p 1583-1600
22. G.C. Sinke, L.C. Walker, F.L. Oetting, and D.R. Stull, Thermodynamic Properties of Aluminum Hydrides, *J. Chem. Phys.,* Vol 47, 1967, p 2759-2761
23. B. Baranowski, M. Tkacz, and S. Filipek, High Pressure Investigations of the Al-H System, in *High Pressure Science and Technology,* Pt. 3, Mater. Res. Soc. Symp. Proc., Vol 22, 1984, p 53-56
24. B. Baranowski, H.D. Hockheimer, K. Strossner, and W. Honle, High Pressure X-ray Investigation of AlH_3 and Al at Room Temperature, *J. Less-Common Met.,* Vol 113, 1985, p 341-347
25. S.K. Konovalov and B.M. Bulychev, High Pressures in the Chemistry of Beryllium and Aluminum Hydrides, *Russ. J. Inorg. Chem.,* Vol 37, 1992, p 1361-1365
26. B. Sundman, B. Jonsson, and J-O. Andersson, The Thermo-Calc Databank System, *CALPHAD,* Vol 9, 1985, p 153-190
27. C. Wolverton, V. Ozolins, and M. Asta, Hydrogen in Aluminum: First-Principles Calculations of Structure and Thermodynamics, *Phys. Rev. B,* Vol 69, 2004, p 144109/1-144109/16
28. Z.D. Popovic, M.J. Stott, J.P. Carbotte, and G.R. Piercy, Theory of the Heat of Solution of Hydrogen in Al and Mg Using Nonlinear Screening, *Phys. Rev. B,* Vol 13, 1976, p 590-602
29. N.A. Johnston and C.A. Sholl, Energy of Hydrogen in fcc Metals, *J. Less-Common Met.,* Vol 103, 1984, p 211-218
30. S. Mahajan and S. Prakash, Heat of Solution of Hydrogen in Aluminum, *Phys. Stat. Sol. (b),* Vol 126, 1984, p 467-480